Calcarenite as a poroelastic granular medium

Nicholas P. Chotiros and Marcia J. Isakson
Applied Research Laboratories,
The University of Texas at Austin,
Austin, TX 78713-802, USA

Abstract- **Calcarenite is described as sand-size particles that are cemented together by carbonates, therefore it should be modeled as a poroelastic medium. Elastic and poroelastic models of calcarenite are compared. The poroelastic models include the baseline Biot model and the Biot-Stoll with contact squirt flow and viscous shear drag (BICSQS) model. Input parameters for the poroelastic models are developed. Reflection loss as a function of frequency and angle is computed. Model predictions of shallow water propagation loss over a calcarenite seabed are compared. Differences in propagation loss predictions are discussed.**

I. INTRODUCTION

The seabed in the southern and western continental shelf of Australia is mainly composed of calcarenite. It is a porous granular medium with cementation. In acoustic studies, it is often treated as an elastic medium [1], with constant compressional and shear wave speeds and attenuations per wavelength. However, calcarenite is characterized as sand-size particles that are cemented together by carbonates. Its physical description indicates that it is a porous medium, containing two phases, a solid sand/carbonate skeletal frame and a pore fluid. Consequently, a poroelastic model would be more appropriate. The starting point is the Biot model [2]. It models the medium as an elastic skeletal frame permeated with a fluid. The loss mechanism in the Biot model is the relative motion between the solid frame and the pore fluid, also known as global flow, and it under-predicts the attenuation observed in sands and sandstones, including calcarenite. Much research has gone into understanding the additional attenuation. Stoll [3] attempted to modify the Biot model by making the frame moduli complex, but such a model has been shown to be non-causal. Another loss mechanism is squirt or local flow. Mavko and Jizba [4] address the squirt flow effects as high and low-frequency asymptotic states. Dvorkin and Nur [5] took a phenomenological approach and proposed a relaxation process associated with squirt flow in response to volumetric strain for sandstone. Murphy, Winkler, and Kleinberg derived a model of the effect of squirt flow in the fluid film at the grain-grain contact on the normal contact stiffness [6]. Mayr and Burkhardt [7] combined the global flow model of Biot with the squirt flow model of Murphy, Winkler, and Kleinberg to produce a more comprehensive model. Chotiros and Isakson [8] included the squirt flow effects on the bulk modulus and combined it with effects of viscous drag in the contact fluid film on the shear modulus, and produced the Biot-Stoll model with contact squirt flow and shear viscous drag (BICSQS). This model contains three relaxation frequencies, the global flow relaxation frequency of the Biot model, a squirt flow relaxation frequency that modifies the frame bulk modulus similar to the Murphy, Winkler, and Kleinberg model also known as the bulk relaxation frequency, and a relaxation frequency associated with the shear drag in the fluid film at the grain-grain contact, also known as the shear relaxation frequency. The BICSQS model has been successfully applied to unconsolidated sandy sediments over a broad frequency range with some success [8], and it is applied to calcarenite as a more physically accurate alternative than the elastic model with constant wave speeds and attenuations per wavelength.

In particular, comparisons will be made to the inverted parameter set obtained by Fan, Duncan and Gavrilov, in the calcarenite column of Table I in Ref. [1]. The values were obtained by inversion from propagation loss measurements. It appears that the shear speed and shear attenuation are most significant, since they control the reflection loss at shallow grazing angles, and the compressional speed was simply set equal to exactly twice the shear speed, and the per wavelength compressional attenuation at one half of the shear attenuation.

II. THEORY

A. Biot's Equations

Biot's equations [3] describe the momentum equilibrium in the solid frame and the pore fluid in a porous medium.

$$\mu\nabla^2 u + (H-\mu)\nabla(\nabla\bullet u) - C\nabla(\nabla\bullet w) = \rho\frac{\partial^2 u}{\partial t^2} - \rho_f\frac{\partial^2 w}{\partial t^2} \quad (1)$$

$$C\nabla(\nabla\bullet u) - M\nabla(\nabla\bullet w) = \rho_f\frac{\partial^2 u}{\partial t^2} - \frac{c\rho_f}{\beta}\frac{\partial^2 w}{\partial t^2} - \frac{F\eta}{\kappa}\frac{\partial w}{\partial t} \quad (2)$$

$$H = \frac{(K_r - K_b)^2}{D - K_b} + K_b + \frac{4}{3}\mu \quad (3)$$

$$C = \frac{(K_r - K_b)}{D - K_b}K_r \quad (4)$$

$$M = \frac{K_r^2}{D - K_b} \quad (5)$$

$$D = K_r\ \ 1+\beta\ \frac{K_r}{K_f} - 1 \quad (6)$$

Work supported by the U.S. Office of Naval Research, Ocean Acoustics Program, grant number N00014-06-1-0125.

978-1-4244-5222-4/10/$26.00 ©2010 IEEE

The momentum equation of the solid frame is given by Eq. (1), and that of the pore fluid in Eq. (2). Both are wave equations. The two equations are coupled by the coefficient C which represents the coupling between the solid and fluid phases through the pore walls. The displacement vector of the frame is u, and that of the fluid v. The parameter w, popularized by Stoll [3], is the difference between u and v scaled by the porosity β: $w=\beta(u-v)$. The elastic parameters C, D, H, and M are defined in terms of the frame shear modulus μ, frame bulk modulus K_b, solid material bulk modulus K_r and fluid bulk modulus K_f in Eqs. (3) to (5). The parameter ρ is the bulk density given by,

$$\rho = (1-\beta)\rho_r + \beta\rho_f \tag{7}$$

where ρ_r and ρ_f are the densities of the solid rock material and the fluid, respectively. The solution may be found in Ref. [3].

In matching a Biot model to the inverted parameters in Ref. [1], a number of input parameters are needed. The parameters are grouped into three groups: Bulk properties, fluid flow and frame response related properties. Under bulk properties, given that the calcarenite is made of calcite particles [9], the bulk modulus and density of the solid grains is taken from tabulated values [10] for calcite. The density is almost exactly 2710 kg/m3, but the bulk modulus is spread over a range of values from 63.7 to 76.8 GPa; a value of 71 GPa was chosen as a representative average value. The porosity of the calcarenite is an issue. If the inverted density was taken at face value, it would indicate a porosity of 0.18. Calcarenites in some Italian formations have porosities that range between 0.21 and 0.52 [11,12]. James and Bone [9], indicated a porosity greater than 0.3 for the Gambier Limestone, a calcarenite formation that runs along the southern margin of Australia. Therefore, in the absence of more precise information, a value of 0.21 will be used for modeling, since it is the smallest of the reported values and the closest to the inverted elastic equivalent. Under the fluid flow related parameters, the viscosity of the pore fluid, i.e. water, is well tabulated and its value is 0.001. The virtual mass term quantifies the effect of the tortuosity of pore spaces. Its value must be between 1 and 3, the former is the limiting value for straight pore tubes and the latter for isotropically tortuous 3-dimensional pores. A value of 1.7 was found to be acceptable for sands [8], and it will be used here in the absence of better information. Permeability is known to be highly variable. From Ref. [9] the measured permeability in the Gambier Limestone varied between 5 and 15 μm^2. Therefore, 10 μm^2 would seem to be a representative value. The pore size a is computed from the permeability κ using the Kozeny-Carman equation, with a Kozeny k_k parameter value of 5, appropriate for spherical grains,

$$\kappa = \frac{\beta a^2}{4k_k} \tag{8}$$

Under frame response, there are just two parameters in the baseline Biot model, the frame bulk and shear moduli. These are impossible to measure directly and they are adjusted to fit the shear and compressional wave speeds. Under the Biot baseline model, they have real values. Following this approach, the parameter values for a Biot model were arrived at, as shown in Table I. The elastic model values from Ref. [1] are also shown for comparison. The elastic model is defined in terms of the bulk density and the speeds and the per wavelength attenuations of the compressional and shear waves. The Biot model is defined in terms of the 11 parameters described above. Having established the bulk and fluid parameters, the frame response parameters were adjusted to fit the Biot model to the elastic model in Ref. [1].

Table I: Parameter values

Parameters		Elastic	Biot	BICSQS
Bulk properties				
Grain density	kg/m^3		2710	2710
Grain bulk mod.	GPa		71	71
Fluid density	kg/m^3		1023	1023
Fluid bulk mod.	GPa		2.375	2.375
Porosity			0.21	0.21
Bulk density	kg/m^3	2400		
Fluid flow				
Viscosity	kg/m-s		0.001	0.001
Virtual mass coef.			1.7	1.7
Permeability	μm^2		10	10
Pore size	μm		30	30
Frame response				
Bulk modulus	GPa		3.8	3.8
Shear modulus	GPa		3.5	3.5
Bulk mod. diff.	GPa			1
Bulk relaxation freq.	kHz			56
Shear relaxation freq.	kHz			150
Wave properties				
Comp. speed	m/s	2426		
Shear speed	m/s	1213		
Comp. att.	dB/λ	0.15		
Shear att.	dB/λ	0.3		

The frame shear modulus in the Biot model was adjusted to give the same shear speed as the elastic model. But it was not possible to match the compressional wave speed. Even with the frame bulk modulus set to zero, the compressional speed was still higher than that of the elastic model. Realizing that propagation loss was controlled by the shear speed, no further attempt was made to match the compressional wave speed. Observing [14] that the Poisson's ratio of the frame of granular sediments is in the region of 0.15, an appropriate value of the frame bulk modulus was computed. The computed wave speeds and attenuations are compared in Figs. 1 and 2.

The most significant difference is in the frequency dependence of the attenuation. The elastic model has a constant attenuation in terms of decibels per wave length, while the Biot model predicts an attenuation that increases with frequency in the frequency range below about 1 kHz. This is a consequence of the loss mechanism being directly related to viscous losses due to the relative motion of the frame and the pore fluid. This is a causal process, whereas the constant attenuation and constant speed assumption in the elastic model is demonstrably non-causal.

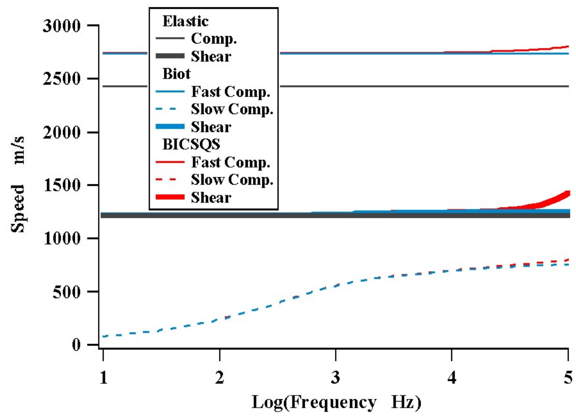

Figure 1. Waves speed as a function frequency.

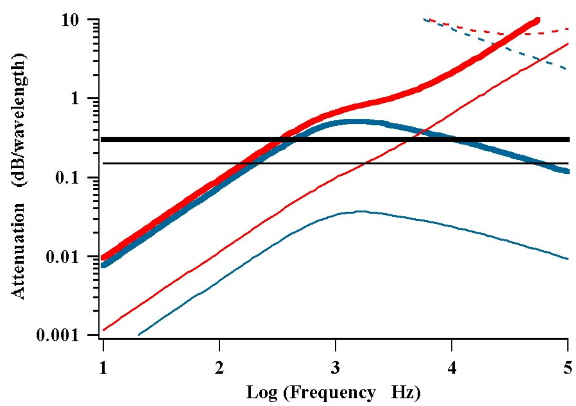

Figure 2. Wave attenuation as a function of frequency.

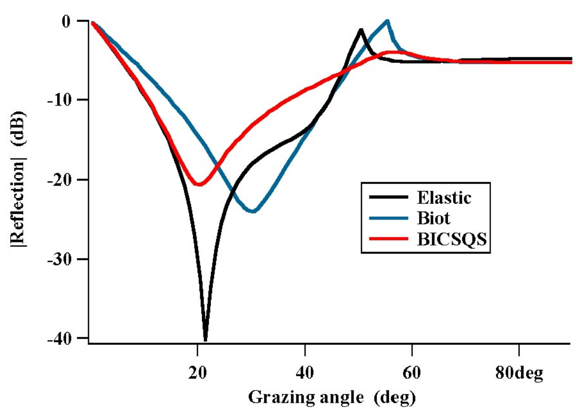

Figure 3. Reflection magnitude as a function of angle.

As an example, the reflection loss at the water/calcarenite interface, at 150 Hz, as a function of grazing angle, are compared in Fig. 3. It shows that the Biot model under estimates the reflection loss at small grazing angles relative to the elastic model. A similar effect has been observed in sands, and the reason is because the Biot model does not include all of the significant loss mechanisms. Stoll [3] attempted to correct the problem by making the frame shear and bulk moduli complex, but that produced a non-causal model similar to the elastic model [15].

Biot's theory predicts two compressional waves, a fast and a slow wave. With a two phase medium, there are naturally two modes of vibration and wave propagation: one in which the solid and fluid move in unison, and the other in which they move in opposite directions. The fast wave is associated with the former and it is the compressional wave for practical purposes. The slow wave is associated with the latter. It is slow and lossy, but it acts as a significant loss mechanism in the reflection coefficient, and therefore should not be ignored.

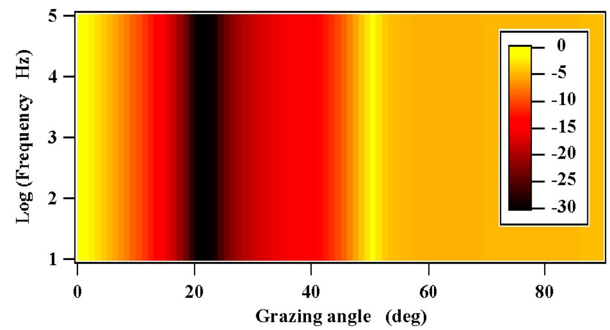

Figure 4. Elastic model: reflection magnitude as a function of angle and frequency.

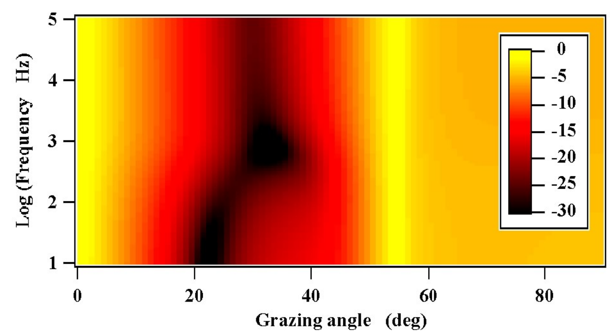

Figure 5. Biot model: reflection magnitude as a function of angle and frequency.

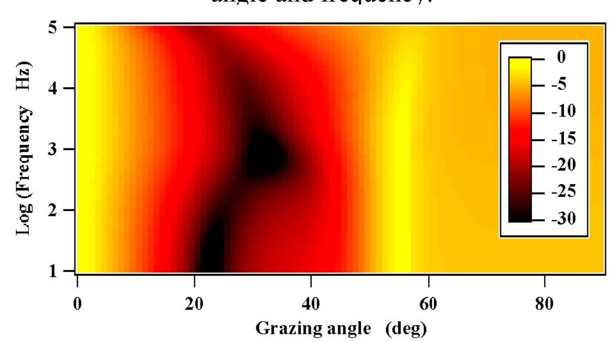

Figure 6. BICSQS model: reflection magnitude as a function of angle and frequency.

B. *BICSQS*

The Biot model underestimates the losses because it was designed for a porous medium with an elastic frame. A granular medium has additional loss mechanisms associated with the grain-grain contact, particularly squirt flow and shear viscous losses. These mechanisms were incorporated in the Biot-Stoll with contact squirt flow and shear viscous drag (BICSQS) model [8]. The parameters for the BICSQS model are shown in the last column in Table I. They are essentially the same as for the Biot model, with the addition of 3 more items. The frame bulk modulus difference and the bulk relaxation frequency are associated with the squirt flow mechanism at the grain-grain contact and they have little effect on the shear wave. For that reason, they have negligible effect on the propagation loss in the calcarenite shallow water. Their values are the ones that were used for sand in Ref. [8] and they are just place holders until the appropriate values for calcarenite are found. The shear relaxation frequency quantifies the effect of viscous drag at the grain-grain contact and it was adjusted to give the desired reflection loss at shallow angles. Thus, the curves for the elastic baseline model and the BICSQS model coincide below 20 degrees in Fig. 3. The value also happens to be the same as the value that worked for sand in Ref. [8].

The reflection loss as a function of frequency and angle are shown in Figs. 4, 5 and 6. The main difference is in the frequency dependence. The elastic model, with constant wave speeds and attenuations per wavelength, produces a plane wave and flat interface reflection loss that is independent of frequency. The poroelastic models show a strong frequency dependence that is the result of the frequency dependence of attenuation and wave speed in all three waves.

III. PROPAGATION LOSS

Using the above models, and assuming an iso-velocity water column, a depth-averaged propagation loss was computed as a function of frequency and range, comparable with the propagation loss plots shown in Ref. [1]. The propagation code was OASES 2.1 [16], with modifications to include the Biot and the BICSQS models. The same water and elastic basement parameters were used as in Ref. [1]. Fig. 7 shows the propagation loss predicted by the elastic model using the same parameter values as Ref. [1]. In Figs. 8 and 9, the Biot and BICSQS models, respectively, were used in the calcarenite layer, with parameter values as given in Table I. Changes were only made to the calcarenite layer.

The horizontal striations in Fig. 7 are evidently due to resonances within the water column, because they persist even when the basement was removed (not shown). Their intensity shows some model dependence. They are strongest in the Fig. 8, under the Biot model, but they are very faint in Fig. 9 under the BICSQS model. The reason for the variations in intensity is not known, particularly since the BICSQS model reflection loss was matched to that of the elastic model at shallow angles. This is a work in progress.

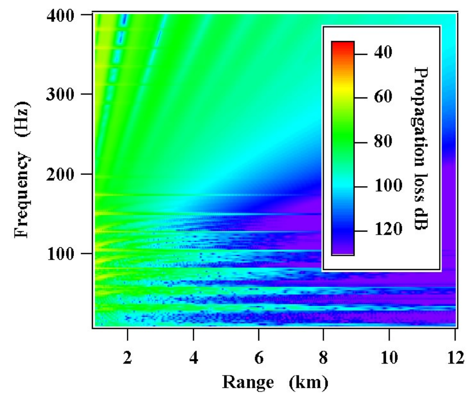

Figure 7. Elastic model: propagation loss

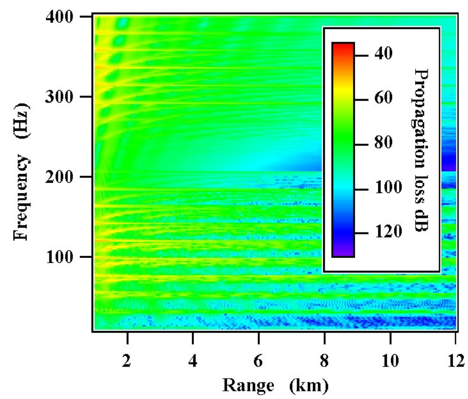

Figure 8. Biot model: propagation loss

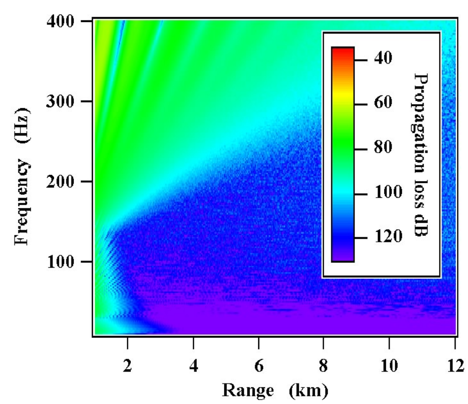

Figure 9. BICSQS model: propagation loss.

IV. DISCUSSION

It is not possible to come to definite conclusions at this stage, but there are interesting points to discuss. The poroelastic models, including the basic Biot model with real frame moduli, and the BICSQS model with grain contact physics, are more complicated than the elastic model. Understandably, there is some reluctance to use them. However, they are more physically realistic, since they include essential physical relationships that one expects to find in the sediment. The parameter values, though many, are not entirely independent, and there is scope for reducing the count.

A number of issues in this study are worth mentioning. The first issue is the uncertainty in the compressional wave speed. Since the propagation loss is most sensitive to the sediment shear wave speed, the inverted compressional wave speed is subject to a large uncertainty. The poroelastic models indicate that the compressional wave speed in the elastic model is physically unlikely. A more likely value is shown in Fig. 1. The second point is the frequency dependence of attenuation. The poroelastic models indicate that the attenuation per wavelength increases with frequency. For compressional waves there is strong experimental evidence [17], but more measurements are needed to test this hypothesis for shear waves. Finally, in a shear dominated environment, the variation of shear speed with depth needs to be investigated because it is well-known that shear speed increases rapidly with depth near the water-sediment interface.

ACKNOWLEDGMENT

The authors would like to thank Alec Duncan for a very useful introduction to the acoustic properties of calcarenite.

REFERENCES

[1] L. Fan, A. J. Duncan, and A. Gavrilov, "Propagation and inversion of airgun signals in shallow water over a limestone seabed," in Underwater Acoustic Measurements: Technologies and Results, 3rd International Conference, Nafplion, Greece, 21-26 June 2009, 2009.

[2] M. A. Biot, "Theory of Propagation of Elastic Waves in a Fluid-Saturated Porous Solid -- I. Low Frequency Range," in J. Acoust. Soc. Am. 28, 168-178, 1956, 1956.

[3] R. D. Stoll, Sediment acoustics, vol. 26. New York: Springer-Verlag, 1989.

[4] G. Mavko and D. Jizba, "Estimating grain-scale fluid effects on velocity dispersion in rocks," Geophysics, vol. 56,1991, pp. 1940-1949.

[5] J. Dvorkin and A. Nur, "Dynamic poroelasticity: A unified model with the squirt and the Biot mechanisms," Geophysics, vol. 58,1993, pp. 524-533.

[6] W. F. Murphy, III, K. W. Winkler, and R. L. Kleinberg, "Acoustic relaxation in sedimentary rocks: Dependence on grain contacts and fluid saturation," Geophysics, vol. 51,1986, pp. 757-766.

[7] S. I. Mayr and H. Burkhardt, "Ultrasonic properties of sedimentary rocks: effect of pressure, saturation, frequency and microcracks," Geophysical Journal International, vol. 164,2006, pp. 246-258.

[8] N. P. Chotiros and M. J. Isakson, "A broadband model of sandy ocean sediments: Biot-Stoll with contact squirt flow and shear drag," J. Acoust. Soc. Am., vol. 116,2004, pp. 2011-2022.

[9] N. P. James and Y. Bone, "Petrogenesis of cenozoic, temperate water calcarenites, south australia: a model for meteoric/shallow burial diagenesis of shallow water calcite sediments," J. Sed. Petrology, vol. 59,1989, pp. 191-203.

[10] G. Mavko, T. Mukerji, and J. Dvorkin, The rock physics handbook. Cambridge, United Kingdom: Cambridge University Press, 1998.

[11] T. Vanorio, C. Scotellaro, and G. Mavko, "The effect of chemical and physical processes on the acoustic properties of carbonate rocks " The Leading Edge, vol. August,2008, pp. 1040-1048.

[12] G. F. Andriani and N. Walsh, "Fabric, porosity and water permeability of calcarenites from Apulia (SE Italy) used as building and ornamental stone," Bulletin of Engineering Geology and the Environment, vol. 62,2003, pp. 77-84

[13] P. C. Carman, "Flow of gases through porous media," in Academic. New York, 1956.

[14] R. Bachrach, J. Dvorkin, and A. Nur, "Seismic velocities and Poisson's ratio of shallow unconsolidated sands," Geophysics, vol. 65,2000, pp. 559-564.

[15] A. Turgut, "An investigation of causality for Biot models by using Kramers-Krönig relations," Shear Waves in Marine Sediments, La Spezia, Italy, October 1990, edited by J. M. Hovem, M. D. Richardson and R. D. Stoll (ISBN0-7923-1357-7, Kluwer Academic, Dordrecht, The Netherlands, 1991),1990, pp. 21-28.

[16] H. Schmidt, "OASES version 2.1, User Guide and Reference Manual," in Department of Ocean Engineering, Massachusetts Institute of Technology, April 30, 1997, 1997.

[17] J.-X. Zhou, X.-Z. Zhang, and D. P. Knobles, "Low-frequency geoacoustic model for the effective properties of sandy seabottoms," J. Acoust. Soc. Am., vol. 125,2009, pp. 2847-2866.